THE AMERICAN SOCIETY OF MECHANICAL ENGINEERS
345 E. 47 St., New York, N.Y. 10017

91-GT-325

A Bulk Flow Model of a Brush Seal System

R. C. HENDRICKS and S. SCHLUMBERGER
NASA Lewis Research Center
Cleveland, Ohio 44135

M. J. BRAUN and F. CHOY
University of Akron
Akron, Ohio 44325

R. L. MULLEN
Case Western Reserve University
Cleveland, Ohio 44106

ABSTRACT

Fibers such as fabric and bristles can be readily fabricated into a variety of seal configurations that are compliant and responsive to high speed or lightly loaded systems. A linear, circular, or contoured brush seal system is a contact seal consisting of the bristle pattern and hardened interface. When compared to a labyrinth seal the brush seal system is superior and features low leakage, dynamic stability, and permits compliant structures. But in turn the system usually requires a hardened smooth interface, permits only limited pressure drops. Wear life and wear debris for operations with static or dynamic excitation are largely undetermined. A seal system involves control of fluid within specific boundaries. The brush and rub ring (or rub surface) form a seal system. In this paper, design similitudes, a bulk flow model, and rub ring (interface) coatings are discussed. The bulk flow model calculations are based on flows in porous media and filters. The coatings work is based on our experience and expanded to include current practice.

1. INTRODUCTION

A seal is the interface between the power stream and structural boundaries. Seals control

(1) Leakage
(2) Dynamics
(3) Tolerance to boundaries
(4) Coolant, lubricant, or emissions flows.

All four affect engine performance through parasitic losses, life, or limit cycles. Current trends toward high-performance, lightweight engines require compliant seal and bearing configurations to accommodate flexible interfaces. The brush seal (linear, circular, or contoured) is one type of seal that permits compliant structures. Circular brush seals by Cross Mfg. Ltd. (Fig. 1) and Rolls-Royce have successfully operated in jet engines for hundreds of hours, Furgeson (1). The leakage can be equivalent to that of several labyrinth cavities, Flower (2) and Gorelov et al. (3), perhaps four to five depending on design and application. However, because the brush is a contact seal, wear and life become concerns (4,5); pressure drop is also limited to prevent bristle blowout and, although seal dynamic perturbations are a major concern, Childs (6) found a four-brush configuration more stable than a labyrinth seal.

Costs of circular brush seals approach $100 per inch of diameter plus tooling; perhaps one-fifth the cost of carbon or labyrinth seals. The cost of a seal system produced by a competent manufacturer approaches $150 per inch of diameter for a 6- to 10-rms surface finish of Al_2O_3, CrO, or magnesium zirconate on a high Ni-based alloy substrate.

Cross Mfg. has also provided linear seal configurations as have other manufacturers. Contoured brush seals currently under investigation are configured to nonlinear boundaries; a major limitation to contouring is convex curvature, which results in excessive porosity at the interface (high leakage).

Brush seal modeling has been limited, ranging from an aperture with the proper flow coefficient to a bulk flow model, Braun (8), to a preliminary numerical model, Mullen et al. (7), to working designs by Cross Mfg., Flower (2).

Visualization studies have been carried out for simulated linear brush configurations in water and oil tunnels, Braun et al. (8-11). The major observed flow patterns were lateral, vortical, rivering, jetting, feather type, endwall, and clearance with strong variations from br stle tip (interface) to the root, see the sketch in Fig. 2. The flows were quantized by using the full-field flow tracking (FFFT) method, Braun et al. (12), which allows qualitative and quantitative flow description before, through, and within the simulated brush seal. Parameters, such as bristle diameter, spacing, voids, length, approach and exit boundaries, and number and spacing of brushes, are under investigation.

Cryogenic brush seal applications have been proposed (13) but turbomachine stability remains a problem (14).

Possible applications of brush seals to automotive applications have also been proposed (15).

Bristle motion strongly influences leakage, dynamics, and modeling, all of which are difficult to

Presented at the International Gas Turbine and Aeroengine Congress and Exposition
Orlando, FL June 3-6, 1991

quantify and apply to the automotive and aerospace industries. Herein we provide a procedure for brush seal system design.

1.1. Nomenclature

A	flow area, wH
a_1, a_2, a_3	reliability, material, and lubricant parameters
C	clearance
$C_{D,0}$	flow coefficient for single aperture
C_F	friction coefficient
C_R	rated load
D_v	volumetric hydraulic diameter
d	bristle diameter
E	Young's modulus
EI	stiffness
e	eccentricity
F_n	normal force (friction)
F_0	equals 1 when $C > 0$ and -1 when $C < 0$
f	friction factor
f_n	natural frequency
f_1	flow area blockage, or bristle overlap, $(1 - P_{or})^3$
f_2	$\sec(\theta + \phi)$
f_3	equals -1 for contacting bristles and 1 for noncontacting bristles
f_4	packing and blooming factor, $1 + 0.05 \frac{\Delta P}{\langle P \rangle}$
f_5	open-channel flow coefficient factor, $C_{D,0} N_x^{-0.4}(1 - 0.8\langle P_x \rangle)A \approx 0.2\ A$
f_6	$\left[\frac{N_\theta - 1 + N_x}{N}\right] \pi d L_0$
G	mass flux (leakage/area)
g	units conversion constant
H	seal dam height (fence height)
I	moment of inertia
L	bristle length
N	number of bristles
N_x	number of bristles in x-direction
N_θ	number of bristles in θ-direction
P_{or}	porosity corrected for bloom and packing
$P_{or,o}$	porosity based on geometry
P_{out}	pressure downstream of seal
ΔP	pressure drop
$\langle P_x \rangle$	$0.5\left(\langle P_x \rangle_1 + \langle P_x \rangle_{N_x}\right)$
$\langle P_x \rangle_1$	$\left[N_x\left(1 + \frac{P_{out}}{\Delta P}\right)\right]^{-1}$
$\langle P_x \rangle_{N_x}$	$\left(1 + \frac{P_{out} N_x}{\Delta P}\right)^{-1}$
Q	volumetric flow rate
R	shaft radius
$(Re)_v$	volumetric Reynolds number
S_L	lateral pitch
S_T	transverse pitch
t_1	compact brush thickness
t_2	brush thickness at H
t_3	brush thickness at interface
$\langle t \rangle$	average brush thickness
V_{open}	open volume
V_{solid}	solid volume
V_{total}	total volume
v	velocity
W	applied load
$w = R\phi_0$	seal width
w_0	preload
w_1, w_2	mass flow rates
x	axial position (along shaft)
y, y_0, y_0'	bristle elastic deformation parameters
$Z_1, \ldots, Z_5$	similitude parameters
z	bristle coordinate
z_a	equivalent aerodynamic load location
β	dynamic rotor angular coordinate
Δ	radial deflection
ε_0	bristle spacing due to manufacturing tolerances
θ	bristle angle; angle position
μ	viscosity

ν	μ/ρ
ρ	density
ϕ	shaft angle to bristle
ϕ_0	reference angle for friction surface, volume and area w/R
ω	rotational speed
$\langle\ \rangle$	average

2. BRUSH SEAL GEOMETRY

A typical jet engine brush seal configuration (Fig. 1), courtesy of Cross Mfg. Ltd.) consists of three elements:

(1) A backing plate (which acts like a sealing dam)
(2) A circumferential or linear set of packed wires (fibers or bristles)
(3) A pinch plate, which plays the role of a retainer for the brush bristles.

The flexibility of the fibers and implicitly the performance of this seal are governed by fiber length, diameter, inclination to the moving surface, packing density, and modulus of elasticity and backing plate clearance (see also similitude parameters in the appendix). Typically, for a circular brush the wire or brush materials are superalloys and range from 0.05 to 0.07 mm (0.002 to 0.0028 in.) in diameter. The bristle is approximately 0.96 mm (0.38 in.) long and aligned at 30° to 50° to the shaft in the direction of rotation. Nominally there are 98 bristles per millimeter (2500 bristles per inch) of circumference. The interface is characterized by a smooth (4 to 16 rms) hardened surface (e.g., Al_2O_3 or CrO).

3. BRUSH SEAL SYSTEM DESIGN

A seal system involves control of fluid within specific boundaries. The brush and rub ring (or rub surface) form a seal system. The brush seal system and its associated loads are illustrated in Fig. 3.

Herein a bulk flow model, rub ring (interface) coatings, and design similitudes are discussed.

3.1. Bulk Flow Model

The bulk flow model calculations are based on Gunter and Shaw (16), which deals with flows in porous media and filters. The coatings work is based on the authors' experience and expanded to include current practice. Preliminary bulk flow models appear in (8) and (15).

Bulk flow model characteristic length. - The major problem in arriving at a conventional type of friction factor - Reynolds number plot is in defining the characteristic length. Gunter and Shaw (16) do this in terms of open volume and friction surface:

$$D_v = 4\,\frac{\text{Open volume}}{\text{Friction surface area}} \tag{1}$$

and Reynolds number becomes

$$(\mathrm{Re})_v = \frac{\rho V D_v}{\mu} = \frac{Q D_v}{A P_{or} \nu} \tag{2}$$

Equation (1) is a hydraulic diameter and allows for nonuniform cross sections.

Friction surface area. - The friction surface depends on how the bristles contact the interface and rub one another. Assuming a fictitious surface at (R + H),

$$\frac{A_f}{N} = (\pi L_0 d - f_6)(1 - f_1) + f_6 + \frac{\left(2 + \frac{H}{R}\right)w(t)}{N} + (f_3 - 1)\pi\frac{d^2}{4}\sec(\theta + \phi) \tag{3}$$

[Bristle surfaces]

+ [Interfaces of (bristle tips, rotor, ficticious)]

The unique feature of brush seals is that most of the flow friction surface lies within the brush itself and the other areas are usually less than 10 percent of the total area. f_1 was estimated from flow observations associated with Braun et al. (11).

Open volume and porosity. - Although the open volume is directly related to porosity, it is difficult to quantize even for simple geometries.

$$V_{open} = V_{total} - V_{solid} = P_{or,o} V_{total} \tag{4}$$

where $P_{or,o}$ is the porosity. For a circular brush with circular bristles

$$V_{open} = \langle t\rangle Hw\left(1 + 0.5\,\frac{H}{R - C}\right) - N\,\frac{\pi d^2}{4}\,L_0 \tag{5}$$

with $[1 - (C/R)] \to 1$. For $C < 0$, it is assumed that bristle deformation is linear and uniform within the brush (and H is diminished by $|C|$). The exact geometric arrangement is not known. For $C > 0$, V_{open} is constant and does not include the clearance volume. (Note that the circumferential spacing change is always $2\pi HN_x/N$.) The bristles are in motion and they both pack and spread, or bloom, (11). From these results an estimate of spread and bloom is related to pressure drop

$$P_{or} = f_4 P_{or,o} \tag{6}$$

Flow calculation. - Brush leakage is the sum of the flow through the bristles and the clearance at the interface between the surface ($R\phi\langle t\rangle$) and the bristle tips.

Brush flow ($C \leq 0$): The empirical relation for friction factor as given in (16) is

$$\frac{f}{2} = \frac{\Delta P g D_v \rho}{10\langle t\rangle G_1^2}\left(\frac{\mu}{\mu_w}\right)^{0.14}\left(\frac{S_T}{D_v}\right)^{0.4}\left(\frac{S_T}{S_L}\right)^{0.6} = \frac{\Phi}{10}\,\frac{\rho\,\Delta P}{G_1^2} \tag{7}$$

where for laminar flows

$$\frac{f}{2} = \frac{90}{(\mathrm{Re})_v} \qquad (\mathrm{Re})_v < 200;\ (\mathrm{Re})_v = \frac{D_v G_1}{\mu} \tag{8}$$

and for turbulent flows

$$\frac{f}{2} = \frac{0.96}{(\mathrm{Re})_v^{0.145}} \qquad w_1 = G_1\langle A\rangle$$

and where S_T is the transverse pitch, S_L is the longitudinal pitch (center to center distances between nearest neighbors in adjacent rows or columns), and μ_w is the viscosity at the wall.

The parameters S_T and S_L are estimated from the brush gometry. For uniform hexagonal packing the number of bristles in the axial and circumferential directions become

$$N_x = \frac{t_1 - d}{H_{t_1}} + 1 \qquad N_\theta = \frac{N}{N_x} \tag{9a}$$

where

$$H_{t_1}^2 \equiv \left(\varepsilon_0 + d\right)^2 - \frac{1}{4}\left[\varepsilon_0 + d\ \sec(\theta + \phi)\right]^2 \tag{9b}$$

and

$$\langle\varepsilon_0\rangle \equiv \frac{w}{N_\theta}\left(1 + \frac{H}{2R}\right)d\ \sec(\theta + \phi) \tag{9c}$$

Then

$$S_T = d\ \sec(\theta + \phi) + \langle\varepsilon_\theta\rangle \tag{9d}$$

$$S_L^2 = \left(\frac{S_T}{2}\right)^2 + H_{t_1}^2 \tag{9e}$$

where $\varepsilon_0 \sim 10^{-4}$ in. represents wire and manufactured packing tolerances.

Channel flow ($C > 0$): Assuming bristle rows to be similar to sequential orifices, the results from Hendricks (17) can be applied, and the axial flow through the clearance with N_x bristle rows becomes

$$G_2 = f_5\sqrt{2\rho\ \Delta P} = \frac{w_2}{wC} \tag{10a}$$

Fence interface ($R + H$): Brush seals have two kinds of edge losses. Both the linear and circular configurations leak at the sealing dam (or fence) and rotor interface. In addition, the linear brush has end wall leakage which is distributed over the circumference of the circular brush forming convergent flow paths along the bristles (divergent for brush on rotor). Flow along channels formed by the bristles and backing washer becomes

$$W_3 = C_{D_3}(Re_3, \Phi)A_3\sqrt{2\rho\ \Delta P} \tag{10b}$$

The flow coefficient is taken from Eq. (7). For flows greater than 0.7 scfm, $W_3 = 0$.

$$C_{D_3}(Re_3, \Phi) = \sqrt{2\,\frac{\Phi}{f}} \tag{10c}$$

$$\approx 0.4 \text{ herein}$$

Flow area ($C < 0$). - When $C < 0$, the average flow area decreases with decreasing porosity and is approximated by

$$\langle A\rangle = \frac{V_{open} f_4}{\langle t\rangle} + A_3 \tag{11a}$$

where A_3 is the flow area at the fence interface ($R + H$),

$$A_3 = N_\theta \frac{d^2}{4}\left[3.732\ \frac{\left(1 + \frac{H}{R - C}\right)}{N_\theta \frac{d}{w}} - \pi\right] \tag{11b}$$

$$D_{V_3} \approx \frac{4A_3}{\left[\pi d + (d + \varepsilon_0)\left(1 + \frac{H}{R}\right)\right]N_\theta} \tag{11c}$$

and for equality use elliptical parimeter.

Flow area ($C > 0$). - When $C > 0$, part of the flow goes through ($\langle A\rangle_{C=0}$), part through A_3, and part passes through the channel of aperture area Cw. The leakage flow is the sum of that through the brush and that through the channel between the bristle tips and the fence interface; rotor and fence interface dynamics are neglected.

The minimum flow area is related to the average bristle spacing.

$$A_{min} = H\left[\left(1 + 0.5\ \frac{H}{R - C}\right)w - N_\theta d\ \sec(\theta + \phi)\right]f_4 \tag{11d}$$

3.2. Bristle Deformation

In a seal the bristles are subject to mechanical, aerodynamic, and pressure drop loads. Relaxation of the prestrained or interference loads permits a restricted movement of the bristle tips that both creates and closes voids and can lead to the onset of instabilities (e.g., fluttering). The aerodynamic load due to the fluid moving along with the rotating interface tends to lift the bristle from the surface into a rub-free state. The load due to longitudinal pressure drop per bristle row flexes the bristles toward the dam or fence. Instabilities of the bristles near the entrance and exit can occur; the bristle deformation increases the leakage area, the packing, and the bloom.

When the bristle tips are not contoured, the bristle tip void areas must also be added to the leakage area.

Bristle tip deformation = H_{def}

= Vector sum (Rotation + Pressure + Preload) displacements

$$= \vec{F}_1\left[\frac{(R\omega)^2}{2},\ F_3\right] + \vec{F}_2(\Delta P,\ F_3) + \vec{F}_3(Z_1)$$

The bristle free length L is the solution of the line representing the bristle, its circular arc, and the shaft. The displaced bristle position and angle with respect to the shaft and the housing is the solution of the free-length arc and the shaft, Appendix A.

3.3. Bristle Response

A simple noninteracting bristle can be considered a cantilever beam with mechanical, aerodynamic, and

pressure drop loadings. The spring load is placed at the tip of the bristle; the aerodynamic load is placed (z_a) from the interface and opposes the spring load, Appendices A and B,

$$z_a = (H + C)\sec(\Theta + \phi)\left[1 + \left(\frac{1}{n + 1}\right)^{1/n}\right] \qquad (12a)$$

an approximation is

$$z_a \simeq 0.5\,\frac{H + C}{n + 1}\,\sec(\Theta + \phi) \qquad (12b)$$

here n is the velocity power law exponent. However, under the pressure drop load the bristle is deflected about the seal dam or fence height and can be considered as a redundant beam with a uniform load. The pressure load is initially considered to act at right angles to the aerodynamic and spring loadings. Bristle stiffness becomes similar to the redundant beam spring constant.

The beam elastic locus, with units L^3/EI can be represented by

$$y = y_0 + y_0'z + \frac{R\langle z - z_0\rangle^3}{6} + S(z) \qquad (13)$$

where y_0 is the deflection at $z = 0$ (at the interface), y_0' is the slope, R is the dimensionless reaction at the propped support, and $S(z)$ is the load function. The spring constant for this case is

$$k = \frac{1}{y_0} \qquad (14a)$$

For the cantilever

$$k = 3\pi EL\,\frac{\left(\frac{d}{L}\right)^4}{64} \qquad (14b)$$

The deformations are assumed to be elastic, and changes in clearance are represented by

$$\Delta C = \Sigma\, y_0 y_0' \qquad (15a)$$

with spring and cross-coupling, Appendix C, related as

$$k_{xx}^{-1} \propto \Sigma\, y_0 \qquad (15b)$$

$$k_{xy} \propto -C_F k_{xx} \qquad (15c)$$

The natural frequency is assumed to be that of a cantilevered steel beam:

$$f_n = \frac{11.3\times10^4}{4L^2}$$

3.4. Bristle Interface Loading

The spring load or preload becomes

$$F_s = k_{xx}L\left[(\Theta + \phi)\Big|_{W+w_0} - (\Theta + \phi)\Big|_{W+w_0=0}\right] \qquad (17)$$

The buckling load is a component of the spring load and is increased by the imposed sliding load if the rotor is reversed; this load is related to the friction coefficient (δ_r is 1 for rotor reversal and -1 otherwise).

$$F_{bk} = \left[\cot(\Theta + \phi) + \delta_r C_F\right]F_s \qquad (18)$$

The buckling displacement is proportional to the direct clearance displacement and equals

$$-\left[-\left(e_s + e_d\right) + C\right]\cos(\Theta + \phi) \qquad (19)$$

when the direct clearance displacement is less than 0 and equals 0 otherwise; e_s and e_d are static and dynamic eccentricities.

Empirically, in terms of Euler column loading or some modifications thereof,

$$\alpha EI\left(\frac{\pi}{L}\right)^2 G\left(\frac{L}{d}\right) \qquad (20)$$

where α is 1/4 for the cantilever and 1/2 for the guided cantilever and $G(L/d)$ are hyperbolic functions. It is important to design the bristles to deform elastically within the seal dynamic limits in order to mitigate fatigue failures and prevent permanent sets (i.e., buckle-before-failure criteria).

3.4. Wear Ring

In order to form an effective seal, a radial preload or interference fit is selected (e.g., 0.13 mm; 0.005 in.). As the shaft rotates, the preloaded brush acts as a cutting wheel; without a suitable protective surface the shaft can suffer thermomechanical damage. Ceramics, such as high density Al_2O_3, ground to surface finishes of 4 to 16 μin. rms have been found to be satisfactory as wear rings. Moderate-density ZrO_2-Y_2O_3 over a NiCrALY bond coat, Mullen et al. (18), has withstood both severe pressure gradients and cryogenic-to-combustion thermal shocking. The bond coat functions as a strain relief and provides significantly higher adhesive/cohesive strengths than other forms of bonding. Laser finishing of the ZrO_2-Y_2O_3 surface can provide higher surface densities for abrasive protection. Typical surfaces are a 0.076-mm (0.003-in.) bond coat and a 0.13-mm (0.005-in.) ceramic plasma sprayed and ground. A similar system formed by chemical vapor deposition but with a 0.025-mm (0.001-in.) bond coat and a 0.076-mm (0.003-in.) ceramic coating could be completed.

Surfaces hardened by metallic coatings, such as nickel chromium plus additives or tungsten carbide, have higher adhesive/cohesive strengths than the ceramics bonded to the substrate. Ion-implanted surface hardening embrittles the surface, and any bristle incursion will score the surface.

In systems requiring heat sinking, a copper band could be inlayed or plated onto the shaft before it is ceramic coated. This process has a great appeal because of the compliance of the copper. For a larger compliance coupling, using a metallic feltmetal pad with the ceramic top coat appears feasible, but functionally gradient materials are better for compactness and thermomechanical behavior, Niino (19).

3.5. Rub Heat Input

The brush is designed to rub the shaft, creating heating, wear, and debris. The objective is to

minimize each. The coating must be smooth and compatible with the bristle material to minimize the interface friction coefficient; the coating must also be capable of passing the generated heat to the working fluid or the system rather than creating a local hot spot as a source of spallation, shaft weakening, and possible instability problems.

A simplistic rub model considers the bristle to be like a commutator brush on an electric motor; the heat input follows as the product of the spring force, the surface velocity, and the interface coefficient.

$$\text{Heat flux} = \frac{C_F F_S V \csc^2(\theta + \phi)}{A_{fs}} \qquad (21a)$$

and using Eqs. (14b) and (17), Eq. (21a) becomes

$$\text{Heat flux} = \frac{3}{16} C_F R\omega Z_2 \qquad (21b)$$

where $A_{fs} = (\pi d^2/4)\sec(\theta + \phi)$ and implicit in C_F is interface lubrication; ($C < 0$).

Figure 4 illustrates the calculated effects of bristle interference on heat flux; the design interference is 0.13 mm (0.005 in.). If the bristles become entangled, their effective stiffness increases and, in turn, significantly increases heat flux. Bristle stiffness also increases as pressure drop increases owing to bristle compaction and forcing of the bristles into the fence gap. The effect is the same as decreasing the bristle length and leads to severe heating, bristle wear, possible spallation of the rub coating, and increased debris generation. For these same reasons the rub-in or burn-in period must be short, and a means of diverting or filtering the debris from the bearings and the coolant passages must be considered.

4. COMPARATIVE RESULTS

The results of flow calculations using the published geometric parameters and volumetric flow rate as a function of clearance data provided by Cross Mfg. Ltd. are compared in Figs. 5 and 6. The deviations at low flows and low pressure drops are evident, to 30 percent. However, the trends and general levels appear correct. In particular, the abrupt flow and pressure changes when the clearance changes from interference to clearance appears physically realistic but does not appear in the Cross data. Although the clearances in Figs. 5 and 6 are initial clearances under no pressure or rotary loading, the calculated values are based on actual or loaded bristle deformations that increase the clearance. The gap widening appears contrary to experimental observations of Ferguson (1) could imply variable rather than constant prop points providing enhanced stiffness. These and other assumptions require further study.

5. DESIGN SIMILITUDES

For single, cantilevered bristles some similitudes include

(1) Load per unit length

$$Z_1 = EL\left(\frac{d}{L}\right)^4$$

(2) Bristle tip pressure

$$Z_2 = \frac{E\left(\frac{d}{L}\right)^2\left(\frac{\Delta}{L}\right)\cos(\theta + \phi)}{\sin^2(\theta + \phi)}$$

(3) Reynolds number

$$Z_3 = \frac{GD_v}{\mu}$$

(4) Interface wear and heating

$$Z_4 = C_F F_n V = C_F V Z_2$$

(5) Fatigue life

$$Z_5 = a_1 a_2 a_3 \left(\frac{C_R}{W + w_0}\right)^n \qquad 2 < n < 3$$

SUMMARY

A bulk flow brush seal model has been developed and is in reasonable agreement with published results from Cross Mfg. Ltd. However, many compromises and assumptions had to be made and their verification remains to be established.

REFERENCES

(1) FERGUSON, J.G. 'Brushes as High Performance Gas Turbine Seals.' Presented at the Gas Turbine and Aero Engine Congress, Amsterdam, The Netherlands, June 8-9, 1988. Sponsored by ASME.

(2) FLOWER, R. 'Brush Seal Development Systems.' Presented at the AIAA/SAE/ASME/ASEE 26th Joint Propulsion Conference, July 16-18, 1990, Orlando, FL. To be published as AIAA Paper 90-2143 (1990).

(3) GORELOV, G.M., REZNIK, V.E., and TSIBILOV, V.I. 'An Experimental Study of the Rate Characteristics of Brush Seals in Comparison With Labyrinth Seals.' Aviatsonnaia Teknika, 4 (1988) 43.

(4) CHUPP, R. 'Evaluation of Brush Seals for Limited Life Gas Turbine Engines.' Presented at the AIAA/SAE/ASME/ASEE 26th Joint Propulsion Conference, July 16-18, 1990, Orlando, FL. To be published as AIAA Paper 90-2140 (1990).

(5) HOLLE, G. and KRISHNAN, M. 'Gas Turbine Engine Brush Seal Applications.' Presented at the AIAA/SAE/ASME/ASEE 26th Joint Propulsion Conference, July 16-18, 1990, Orlando, FL. To be published as AIAA Paper 90-2142 (1990).

(6) CONNER, K.J. and CHILDS, D.W. 'Brush Seal Rotordynamic Damping Characteristics.' Presented at the AIAA/SAE/ASME/ASEE 26th Joint Propulsion Conference, July 16-18, 1990, Orlando, FL. To be published as AIAA Paper 90-2139 (1990).

(7) MULLEN, R.L., BRAUN, M.J., and HENDRICKS, R.C. 'Numerical Modeling of Flows in Simulated Brush Seal Configurations.' Presented at the AIAA/SAE/ASME/ASEE 26th Joint Propulsion Conference, July 16-18, 1990, Orlando, FL. To be published as AIAA Paper 90-2141 (1990).

(8) BRAUN, M.J., HENDRICKS, R.C., and CANACCI, V.A. 'Non-Intrusive Qualitative and Quantitative Flow Characterization and Bulk Flow Model for Brush Seals.' Presented at the International Tribology Conference, Nagoya, Japan, 1990.

(9) BRAUN, M.J., HENDRICKS, R.C., and CANACCI, V.A. 'Flow Visualization in a Simulated Brush Seal.' Presented at the ASME GasTurbine Conference, Brussels, Belgium, 1990.
(10) BRAUN, M.J., HENDRICKS, R.C., and CANACCI, V.A. 'Flow Visualization and Quantitative Velocity and Pressure Measurements in Simulated Single and Double Brush Seals.' Presented at the STLE 1990 Annual Meeting, Denver, Colorado, May 7-10, 1990.
(11) BRAUN, M.J., CANACCI, V.A., and HENDRICKS, R. 'Flow Visualization and Motion Analysis for a Series of Four Sequential Brush Seals.' Presented at the AIAA/SAE/ASME/ASEE 26th Joint Propulsion Conference, July 16-18, 1990, Orlando, FL. To be published as AIAA Paper 90-2482 (1990).
(12) BRAUN, M.J., IDA, N., BATUR, C., ROSE, B., HENDRICKS, R.C., and MULLEN, R.L. 'A Non-Invasive Laser Based Method in Flow Visualization and Evaluation in Bearings,' in International Conference on Tribology -- Friction, Lubrication and Wear Fifty Years On. (The Institution of Mechanical Engineers, London, Great Britain, 1987) Paper C 347/143, p. 37.
(13) HENDRICKS, R.C., BRAUN, M.J., and MULLEN, R.L. 'Brush Seal Configurations for Cryogenic and Hot Gas Applications.' Presented at the 1990 Conference on Advanced Earth-to-Orbit Propulsion Technology, NASA Marshall Space Flight Center and University of Alabama-Huntsville, Huntsville, Alabama, May 15-17, 1990.
(14) von PRAGNEAU, G. 'Special Presentation;' Session 106-ASME23 Rocket Engine Turbomachinery Instabilities. Presented at the AIAA/SAE/ASME/ASEE 26th Joint Propulsion Conference, July 16-18, 1990, Orlando, FL.
(15) HENDRICKS, R.C., BRAUN, M.J., CANACCI, V.A., and MULLEN, R.L. 'Brush Seals in Vehicle Tribology.' Presented at 1990-Leeds/Lyon Symposium, Leeds England, Sept. 1990.
(16) GUNTER, A.Y. and SHAW, W.A. 'A General Correlation of Friction Factors for Various Types of Surfaces in Crossflow.' ASME Trans., 67 (1945) 643.
(17) HENDRICKS, R.C. 'Three-Step Labyrinth Seal for High-Performance Turbomachines.' NASA TP-1848 (1987).
(18) MULLEN, R.L., PADOVAN, J., BRAUN, M.J., CHUNG, B.T.F., McDONALD, G., and HENDRICKS, R.C. 'Thermomechanical Design Criteria for Ceramic-Coated Surfaces.' NASA TM-87328 (1986).
(19) DR. NIINO, Private communication. To be presented at the Functionally Gradient Materials Symposium, Tokyo, Japan, Oct. 8-9, 1990.
(20) IWINSKI, T. 'THEORY OF BEAMS', Pergamon Press, 1958.

APPENDIX A

BRISTLE LENGTH, DISPLACEMENTS, AND DEFORMATIONS

Bristle Length

The free bristle length (L) for bristles with cross section length, $L_1|_{C=0}$, and angle θ (Fig. 3) can be approximated from the solution of the equations,

$$z - R_1 = \tan\left(\theta - \frac{\pi}{2}\right)x$$

$$\left(z - R_1\right)^2 + x^2 = \ell_2^2$$

$$z^2 + x^2 = R^2$$

where

$$R_1 = R + \ell_1 ,$$

$$\ell_1 = L_1\Big|_{C=0} ,$$

and

$$\ell_2 = L$$

The actual length depends also on the tip shape and wear and the length, L, represents a contoured tip with no wear. When the clearance is greater than zero, the free length represents the undeformed bristle length.

Bristle Displacements

When the clearance is less than zero, the bristle is displaced and spring loaded against the interface (seal preload). The change in angle θ and intersection or rub point can be calculated from

$$\left(z_1 - R_1\right)^2 + x_1^2 = \ell_2^2$$

$$z_1^2 + x_1^2 = (R + C)^2$$

$$\Delta\theta = \tan^{-1}\left|\left(\frac{x_1}{z_1 - R_1}\right)\right| - \theta$$

$$\Delta\phi = \tan^{-1}\left(\frac{x_1}{z_1}\right) - \phi$$

While this change in angle does not change the fiber or bristle length it does change the effective prop or restraining point of the bristle relative to the backing plate or washer.

Bristle Deformations

The modeled loading is assumed to be the vector sum of (1) preload, (2) pressure drop, and (3) rotation fluid dynamics with attempts to handle interbristle friction support by imposing a propped point on an otherwise simple cantilever beam. The actual bristle interference, lateral support, and torsional effects are not known; the authors have observed bristle sliding by comparing photographs and video tape of brush displacements but have not quantized these results. The elastic axes for bristle deformations (Fig. 3) are assumed linear and additive with pressure drop in the axial-radial plane and preload and rotation effects in the circumferential-radial plane. For this paper, it is assumed that the propped points are scaled by fence height (sealing dam); actually separate scales should be used for each plane.

Assumed Prop Locations

(1) Axial-radial plane
Prop distance = 1.15 fence height
(2) Circumferential-radial plane
Prop distance = 1.5 fence height

The elastic axis was determined using the methods of Iwinski (20). The interference deflection is assumed known, and the load unknown. The elastic locus is normalized in terms of the unknown load (P) and the stiffness B = EI. Here, L is bristle length, S is load function (20), c is prop point, R is propped support reaction force, P is concentrated load or force, W is load per unit length, y is deflection, and x is beam coordinate starting at the free end.

$$\frac{By}{P} = y_0 + y_0'x + \left(\frac{R}{6P}\right)(x - c)^3 + S(x)$$

where c is the prop point and

$$S(x) = \frac{(x - c)^3}{6}$$

With the boundary conditions

$$y(L) = y'(L) = y(c) = 0$$

solutions for

$$y_0,\ y_0',\ \text{and}\ \frac{R}{P}$$

become,

$$\frac{R}{P} = \frac{3}{(L - c)^2}\left[\frac{S(L) - S(c)}{(L - c)} - S'(L)\right]$$

$$y_0 = \frac{Rc}{2P}(L - c)^2 + cS'(L) - S(c)$$

$$y_0' = -\frac{R}{2P}(L - c)^2 - S'(L)$$

Concentrated Load (P) Located at (g)

$$S(x) = \frac{(x - g)^3}{6}$$

Uniform Load (W) Over the Interval (a,b)

$$S(x) = \left[\frac{(x - a)^4}{24} - \frac{(x - b)^4}{24}\right]\left(\frac{W}{P}\right)$$

Once the bristle position has been determined, the actual deflection y_0 is known. With $g = 0$, the load P can be determined at the tip of the bristle. This load is important as it relates to wear and heating while y_0 provides a measure of bristle dynamic stiffness.

The brush pressure drop divided by number of bristles in the axial direction provides a measure of bristle loading. The load W per unit length of bristle can be assigned and the deflection calculated.

Aerodynamic lifting loads occur from several sources including nonuniform pressure field surrounding skewed cylinders in cross flow (inclined at an angle $(\Theta + \phi)$), from Couette flows over the bristle tips providing a fluid film effect (bearings), and fluid rotation or preswirl into the seal pack due to shaft motion. These forces, in turn, are complicated by surface effects commonly labeled friction, asperity contacts, and fluid surface tension within the pack. These details are the subject of ongoing work.

APPENDIX B

PRESWIRL AERODYNAMIC LOAD

While the velocity profile within the brush is unknown we approximate it, from low rpm observations without substantiation, as

$$\frac{u}{u_0} = \left(1 - \frac{z}{L_a}\right)^n$$

where $u_0 = R\omega$, $n \sim 10$, and $L_a = L + C$.

The average velocity becomes

$$\left\langle\frac{u}{u_0}\right\rangle = \frac{1}{n + 1}$$

and is located at

$$\frac{z}{L_a} = 1 - \left(\frac{1}{n + 1}\right)^{1/n}$$

The aerodynamic load becomes

$$F = \frac{C_D}{2}\rho\left\langle\frac{u}{u_0}\right\rangle^2 u_0^2\, Ld$$

where

$$Re < 3.2 \qquad C_D = \frac{10}{Re^{3/4}}$$

$$3.2 < Re < 10^3 \qquad C_D = \frac{5.6}{Re^{1/4}}$$

$$10^3 < Re < 10^4 \qquad C_D = 1$$

$$Re = \frac{\rho u_0 d}{\mu}$$

APPENDIX C

BRUSH FORCES AND STIFFNESS

Assume that clearance $C < 0$ for $0 < \beta < 2\pi$ and changes in clearance are given by

$$\Delta = e\cos(\beta + \phi) + C$$

$$= e\cos\zeta + C$$

Summing the vertical forces

$$F_{yx} = \int_0^{2\pi}(W\sin\zeta + WC_F\cos\zeta)(C + e\cos\zeta)d\zeta$$

$$= \pi C_F eW$$

where

$$W = N_x f_7 \frac{3\pi}{64}\frac{Ed^2}{C}\left(\frac{d}{\ell_e}\right)^2\left(\frac{C}{\ell_e}\right)\csc^2(\Theta + \phi)$$

and since the pinning conditions are unknown we approximate,

$$\ell_e \sim \frac{L}{3}$$

and from bristle packing, increasing the moment of inertia $(I/I_o) = 20$

$$f_7 = 20$$

Summing the horizontal forces

$$F_{xx} = \int_0^{2\pi} (W \cos \zeta + WC_F \sin \zeta)(C + e \cos \zeta)d\zeta$$

$$= \pi eW$$

For a displacement in the vertical direction

$$\Delta = C + e \cos\left(\zeta - \frac{\pi}{2}\right) = e + e \sin \zeta$$

Summing the vertical forces

$$F_{yy} = \int_0^{2\pi} (W \sin \zeta + WC_F \cos \zeta)(C + e \sin \zeta)d\zeta$$

$$= \pi eW$$

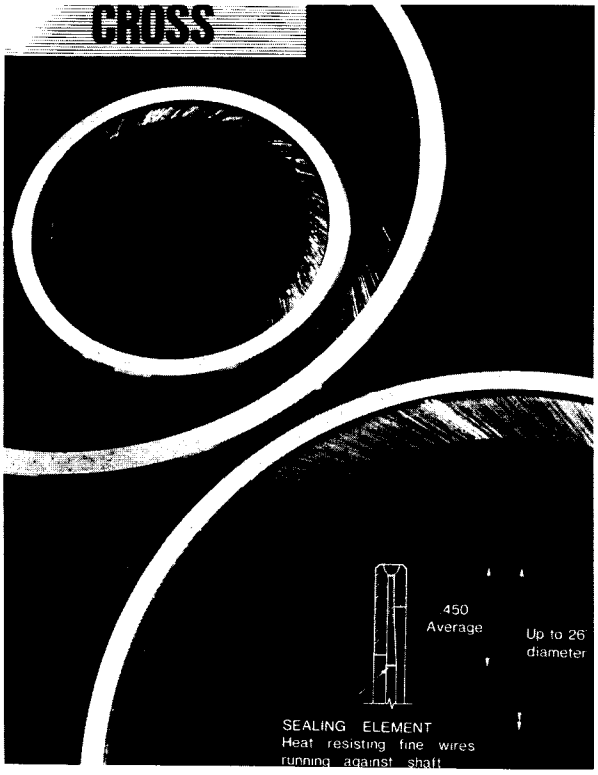

FIGURE 1. - CIRCULAR BRUSH SEAL (COURTESY OF CROSS MFG. LTD.)

Summing the horizontal forces

$$F_{xy} = \int_0^{2\pi} (W \cos \zeta + WC_F \sin \zeta)(C + e \sin \zeta)d\zeta$$

$$= -\pi C_F eW$$

The direct and cross coupled stiffness promoted by the brush acting on the rotor becomes

$$K_{xx} = K_{yy} = \pi W$$

$$K_{yx} = -K_{xy} = \pi C_F W$$

and provides a stabilizing influence on rotor dynamics.

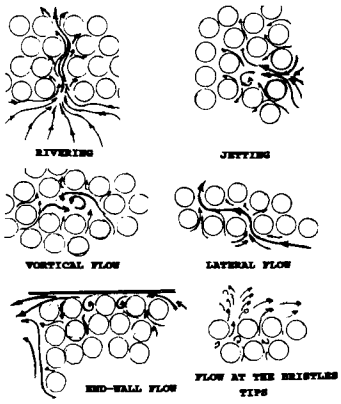

FIGURE 2. - "OBSERVED FLOW PATTERNS".

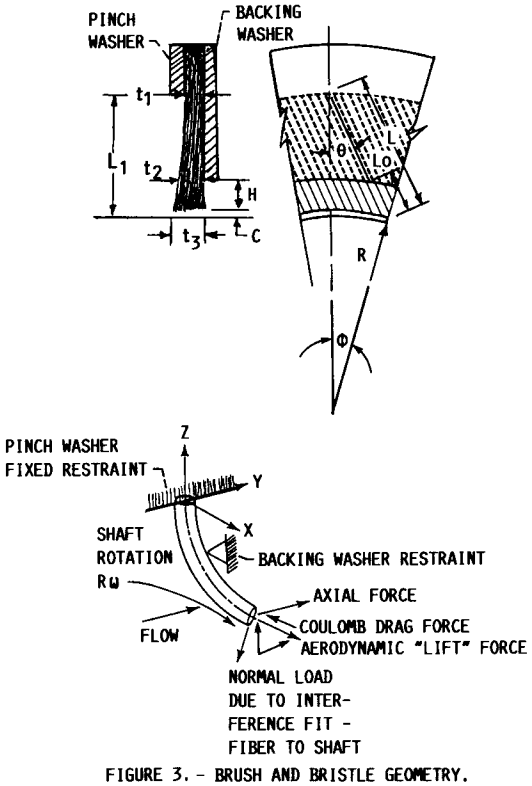

FIGURE 3. - BRUSH AND BRISTLE GEOMETRY.

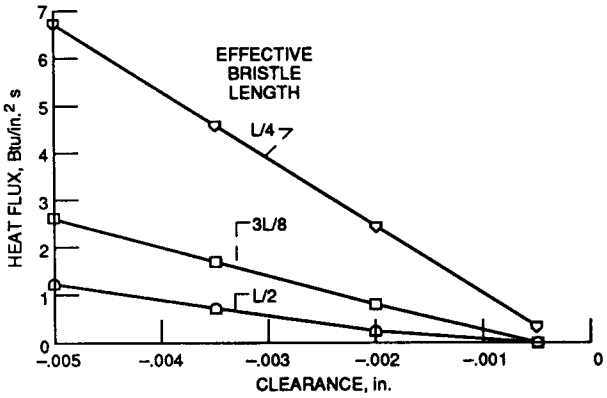

FIGURE 4. - HEAT FLUX VERSUS CLEARANCE WITH EFFECTIVE BRISTLE LENGTH AS A PARAMETER.

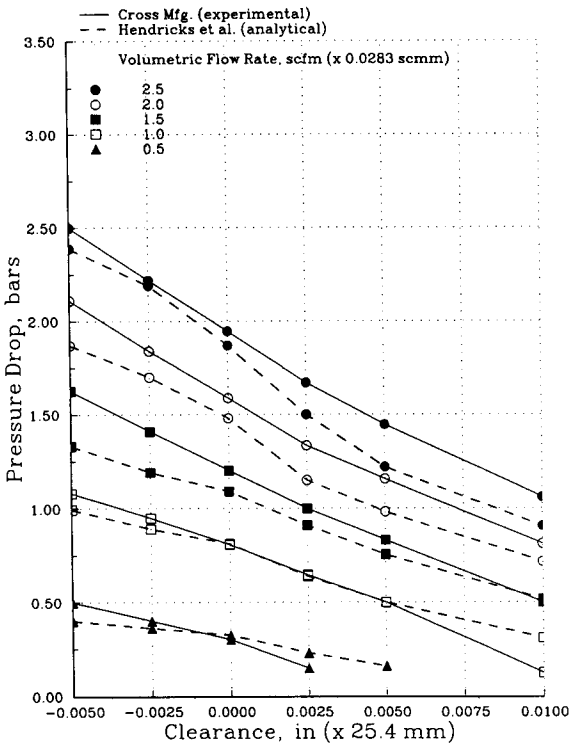

FIGURE 5. - BULK FLOW MODEL PRESSURE VERSUS NO FLOW CLEARANCE. COMPARISON WITH CROSS MFG. LTD. DATA SHEET.

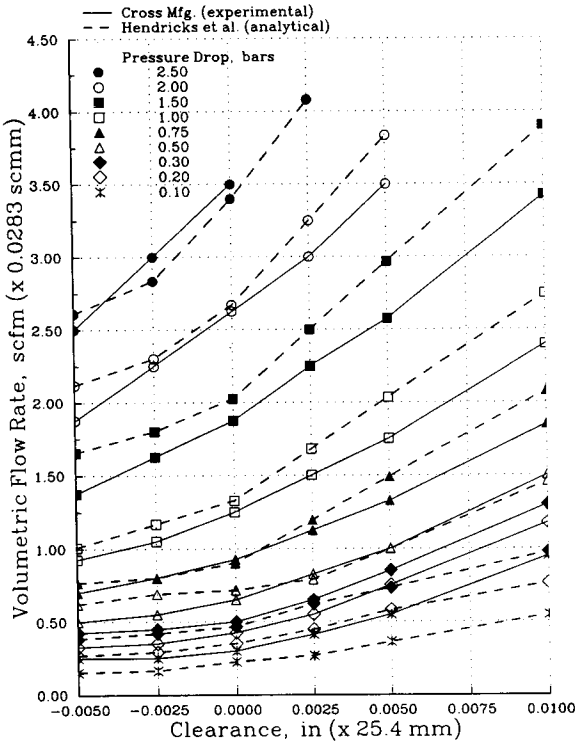

FIGURE 6. - BULK FLOW MODEL VOLUMETRIC FLOW RATE VERSUS NO FLOW CLEARANCE. COMPARISON WITH CROSS MFG. LTD.